

# Carboxy-functionalized Multi-Walled Carbon Nanotubes Hybridized with Poly(Xanthurenic Acid) Enhance the Electrocatalytic Oxidation of Ascorbic Acid, Dopamine, and Uric Acid

Kuo-Chiang Lin, Ying-Sheng Li, Shen-Ming Chen \*

Electroanalysis and Bioelectrochemistry Lab, Department of Chemical Engineering and Biotechnology, National Taipei University of Technology, No.1, Section 3, Chung-Hsiao East Road, Taipei 106, Taiwan (ROC).

\*E-mail: [smchen78@ms15.hinet.net](mailto:smchen78@ms15.hinet.net)

Received: 21 November 2014 / Accepted: 8 January 2015 / Published: 19 January 2015

---

Glassy carbon electrodes (GCEs) were modified with different types of hybrid composites prepared from poly(xanthurenic acid), single-walled carbon nanotubes (SWCNT), and multi-walled carbon nanotubes (MWCNT). They were studied with respect to the simultaneous determination of ascorbic acid (AA), dopamine (DA), and uric acid (UA). The hybrid composite GCE displays a relatively low overpotential and high current response for the analytes. Differential pulse voltammetry (DPV) shows good selectivity and a linear response in the concentration ranges of 10  $\mu\text{M}$ –2.3 mM, 5  $\mu\text{M}$ –165  $\mu\text{M}$ , and 5  $\mu\text{M}$ –1.65 mM for AA, DA, and UA, respectively. The sensitivities are 145.8, 2036.8, and 338.6  $\mu\text{A mM}^{-1} \text{cm}^{-2}$ , and the detection limits are 10  $\mu\text{M}$ , 1  $\mu\text{M}$ , and 5  $\mu\text{M}$  (at an S/N of 3). The method was successfully applied to the determination of the three species in spiked urine samples.

---

**Keywords:** Ascorbic acid, Dopamine, Uric acid, Xanthurenic acid, Single-walled carbon nanotube, Multi-walled carbon nanotube

## 1. INTRODUCTION

Ascorbic acid (AA), dopamine (DA), and uric acid (UA) usually coexist in biological samples. The development of a selective and sensitive method for simultaneous determination of AA, DA, and UA is highly desirable for analytical application and diagnostic research. Among the various analytical methods, electrochemical sensors offer several advantages such as small size of electrode, possibility of *in situ* measurements and requirement of small amount of the sample [1–3].

In recent years, voltammetric techniques for the detection of AA, DA, and UA have attracted considerable interest due to their fast response and high sensitivity. However, a key problem encountered is the overlap of the peak potentials for these three species at conventional electrodes with the pronounced fouling effect, resulting in poor selectivity and reproducibility [4]. To overcome the above problems, various electrode-modified materials such as metal nanoparticles [3,5], organic redox mediators [6,7], polymers [8–10], carbon nanofibers [11,12], graphene [12], and carbon nanotubes (CNTs) [13] were used to improve the selectivity. Among these electrodes, carbon material based electrode is considered as one of the most effective electrodes to carry out the simultaneous determination of AA, DA, and UA due to their remarkable electrocatalytic properties.

Xanthurenic acid (Xa) is a product of the tryptophan–NAD pathway. It is related to various pathological conditions [14–16], although the biological function of this compound remains obscure [17]. Xa acts as a potent iron chelator and has been shown to have prooxidant actions [17]. This compound can form a variety of possible dimers after oxidation, leading to radicals or cations, which can couple with phenoxy radicals, with other dimer radicals or with unconverted compounds to produce polymers adhering strongly to the electrode surface, as evidenced for other phenols [18,19]. Therefore, an investigation into the use of the Xa-modified electrode to oxidize biologically important biological compounds, especially AA, DA and UA, is a worthwhile endeavor [20–28].

In this work, functionalized CNTs and Xa are used to design an active hybrid composite. Hybrid types are characterized and investigated for simultaneous determination of AA, DA, and UA by cyclic voltammetry, scanning electron microscopy, amperometry, and differential pulse voltammetry.

## 2. MATERIALS AND METHODS

### 2.1. Reagents

Single-walled carbon nanotubes (SWCNT), multi-walled carbon nanotubes (MWCNT), xanthurenic acid (Xa), ascorbic acid (AA), dopamine (DA), and uric acid (UA) were purchased from Sigma-Aldrich Chemical Co. (St. Louis, MO, <http://www.sigmaaldrich.com/>). All other chemicals (Merck Co., Darmstadt, Germany, <http://www.merckgroup.com/en/index.html>) used were of analytical grade (99%). Double distilled deionized water was used to prepare all the solutions. A phosphate buffer saline (PBS) of pH 7 was prepared using  $\text{Na}_2\text{HPO}_4$  (0.05 M) and  $\text{NaH}_2\text{PO}_4$  (0.05 M).

### 2.2. Apparatus

All electrochemical experiments were performed using CHI 1205a potentiostats (CH Instruments, USA). A glassy carbon electrode (GCE) was purchased from Bioanalytical Systems (BAS) Inc. (<http://www.basinc.com/products/ec/sve.php>), USA. The GCE was used with diameter of  $\phi = 0.3$  cm (exposed geometric surface area of  $A = 0.0707$  cm<sup>2</sup>) for all electrochemical techniques except of amperometry ( $\phi = 0.6$  cm;  $A = 0.2826$  cm<sup>2</sup>). Prior to modification, the GCE was well polished with

the help of BAS polishing kit with aqueous slurries of alumina powder (0.05  $\mu\text{m}$ ), rinsed and ultrasonicated in double distilled deionized water (18.3  $\text{M}\Omega\text{ cm}$ ) for 3 min. The ADVANTEC (HONG I Instruments Co., Taipei, Taiwan, <http://www.hongi-ins.com.tw/>) filter (porosity = 1  $\mu\text{m}$ ) was used to purify all functionalized CNTs. A conventional three-electrode system which consists of an Ag/AgCl (saturated KCl) reference electrode, a bare GCE or CNTs/GCE or polyXa/GCE or CNTs-polyXa/GCE working electrode, and a platinum wire counter electrode, was used. The electrochemical cells were kept properly sealed to avoid the oxygen interference from the atmosphere. The buffer solution was entirely altered by deaerating using nitrogen gas atmosphere. Morphological characterization of composites was examined by means of scanning electron microscopy, SEM (S-3000H, Hitachi, Japan, <http://www.hitachi-hitec.com/global/em/>). For our convenience, ITO substrates were used for SEM analysis.

### 2.3. Preparation of different polymer-CNTs hybrid types

All CNTs including SWCNT and MWCNT were functionalized with carboxylic group according to our previous method [29]. Xa was the monomer used to prepare the polymer (polyXa) by electropolymerization using GCE or CNTs/GCE electrode in 0.1 M  $\text{H}_2\text{SO}_4$  (pH 1.5) containing  $10^{-2}$  M Xa monomers. The polyXa-CNTs hybrid composites were prepared in two procedures including the adsorption of CNTs and the electropolymerization of Xa. They were arranged in two hybrid types and denoted as polyXa/CNTs and CNTs/polyXa corresponding to the polyXa formation before/after the CNTs adsorption.

## 3. RESULTS AND DISCUSSION

### 3.1. Characterization of polyXa-CNTs hybrid films

Fig. 1 shows the cyclic voltammograms of different modified electrodes in pH 7 PBS. Fig. 1A displays the voltammograms of CNTs/polyXa film type including (a) polyXa, (b) SWCNT/polyXa, and (c) MWCNT/polyXa. Fig. 1B displays the voltammograms of polyXa/CNTs film type including (a) polyXa, (b) polyXa/SWCNT, and (c) polyXa/MWCNT. Both CNTs/polyXa and polyXa/CNTs hybrid film types maintain the polyXa redox couple with slightly potential shift and small peak-to-peak separation except of peak current. It means that the electron transfer process is not changed after hybridization. One can see that redox peak currents are enhanced by CNTs especially for MWCNT-hybrid composites due to high active surface area. Particularly, the polyXa/MWCNT (Fig. 1B(c)) shows higher current than MWCNT/polyXa (Fig. 1A(c)) in the potential range of -0.2–0.05 V. This phenomenon might be caused by the compact hybrid structure consisted of the polyXa (covalent bonding) in first layer and the MWCNT in second layer. It provides a hint that the immobilized procedure of first polyXa and second CNTs is the suitable arrangement for the preparation of polymer-CNTs hybrid nanocomposites. Moreover, both two types of hybrid nanocomposites have good agreement in the formal potential with the related works [30,31]. It indicates that the hybrid nanocomposite types maintain the electrochemical behaviors of the electroactive polyXa species.

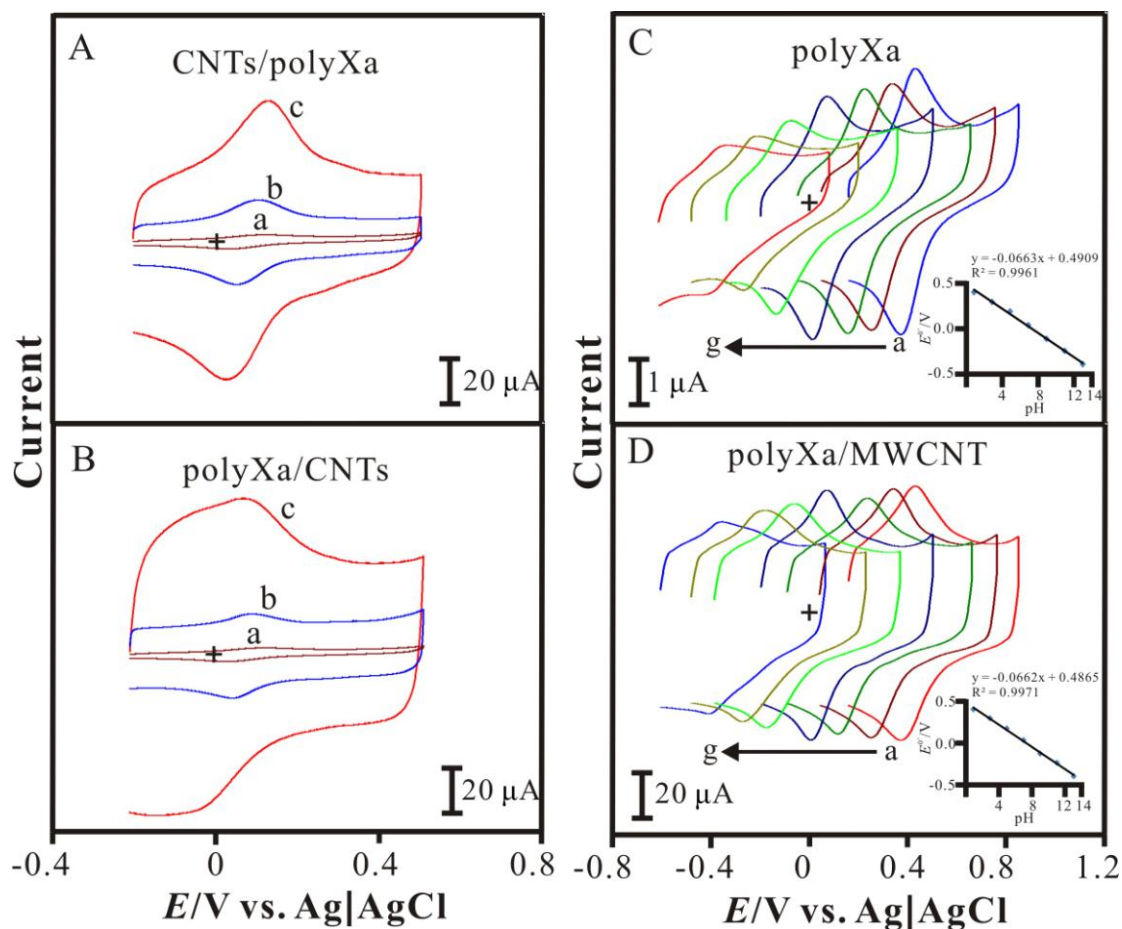


**Figure 1.** CVs of various CNTs-polyXa types including (A) the CNTs/polyXa type of: (a) polyXa, (b) SWCNT/polyXa, (c) MWCNT/polyXa; and (B) the polyXa/CNTs type of: (a) polyXa, (b) polyXa/SWCNT, (c) polyXa/MWCNT, examined in pH 7 PBS. CVs of (C) polyXa/GCE and (D) polyXa/MWCNT/GCE examined in different pH conditions of (a) pH 1, (b) pH 3, (c) pH 5, (d) pH 7, (e) pH 9, (f) pH 11, and (g) pH 13, respectively. Scan rate =  $0.1 \text{ Vs}^{-1}$ .

Fig. 1C & D displays the pH-dependent voltammetric response of polyXa and polyXa/MWCNT modified electrodes. The formal potential ( $E^{0'}$ ) shifts negatively as the pH value of the solution increases. It is pH-dependent, electroactive, and stable in different pH conditions. Considering the correlation between  $E^{0'}$  and pH in the range of pH 1–13, it exhibits a linear equation as  $E^{0'}(\text{mV}) = -0.0663\text{pH} + 0.49$  ( $R^2 = 0.9961$ ) and  $E^{0'}(\text{mV}) = -0.0662\text{pH} + 0.49$  ( $R^2 = 0.9971$ ) for polyXa and polyXa/MWCNT, respectively. One can know that almost the same slope values of  $-66.3 \text{ mV pH}^{-1}$  and  $-66.2 \text{ mV pH}^{-1}$  for both modifiers. They are close to that given by the Nernstian equation for equal number of protons and electrons transfer processes, indicating two protons and two electrons transfer in the electrochemical system. This result is corresponding to that has been reported [30,31]. One can also know that the CNTs enhance the current response but do not affect the polyXa redox process in the hybrid composite.

Fig. 2A-C shows the cyclic voltammograms for polyXa/GCE, polyXa/SWCNT/GCE, and polyXa/MWCNT/GCE examined with different scan rate in pH 7 PBS. All of them exhibit one similar redox couple but different average formal potential at  $E^{0'} = +0.094 \text{ V}$ ,  $E^{0'} = +0.082 \text{ V}$ , and  $E^{0'} =$

+0.072 V for polyXa, polyXa/SWCNT, and polyXa/MWCNT, respectively. Both anodic and cathodic peak currents are directly proportional to scan rate up to  $100 \text{ mV s}^{-1}$  (insets of Fig. 2) as expected for surface-confined and stable redox process. This also indicates that the surface-controlled process in the electrochemical system. The observation of well-defined and persistent cyclic voltammetric peaks indicates that the polyXa/GCE and polyXa/MWCNT/GCE exhibit electrochemical response characteristics of redox species confined on the electrode.

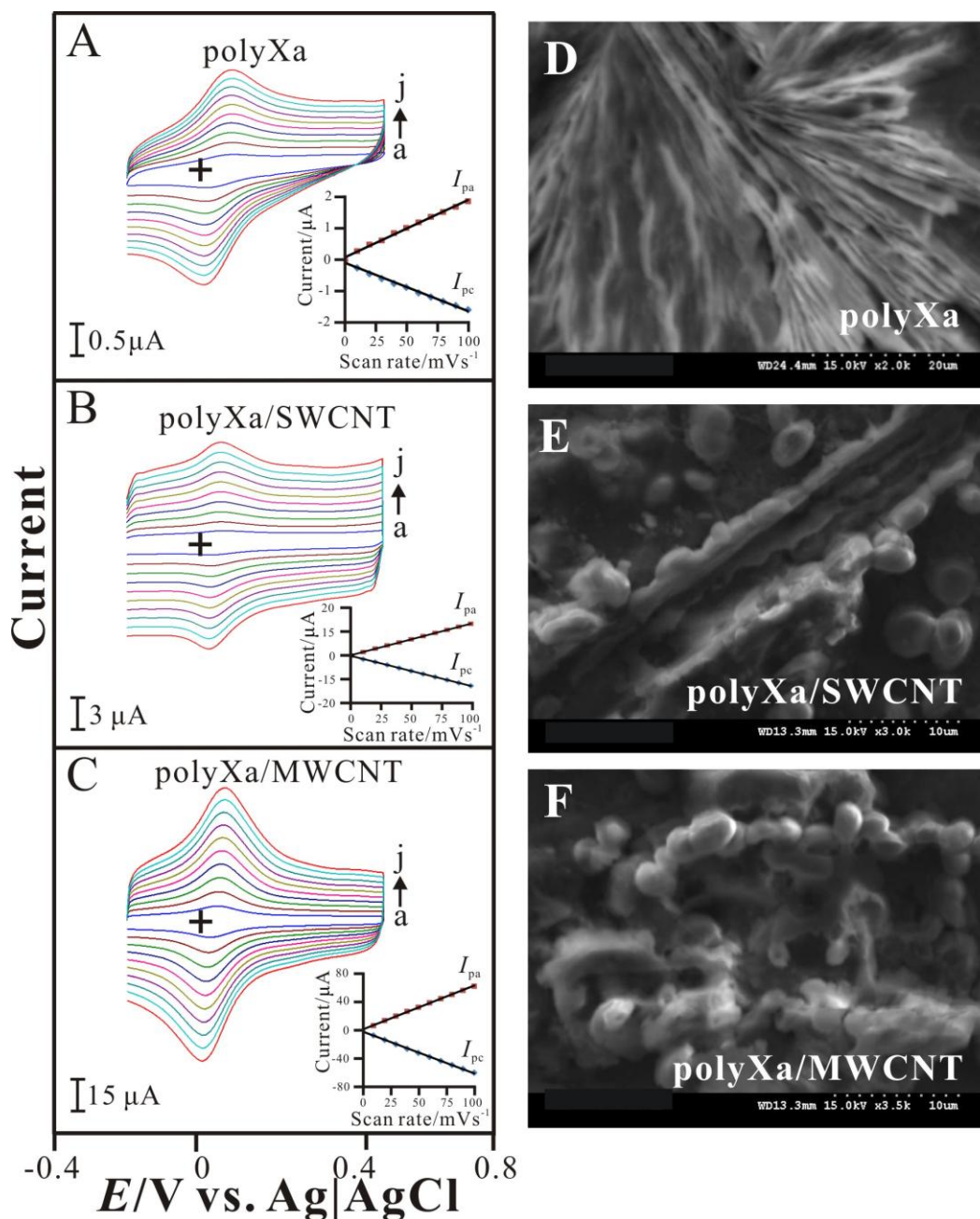


**Figure 2.** CVs of (A) polyXa/GCE, (B) polyXa/SWCNT/GCE, and (C) polyXa/MWCNT/GCE examined in 0.1 M PBS (pH 7) with various scan rates of (a) 10, (b) 20, (c) 30, (d) 40, (e) 50, (f) 60, (g) 70, (h) 80, (i) 90, (j)  $100 \text{ mV s}^{-1}$ , respectively. Insets: the plots of the peak current ( $I_p$ ) vs. scan rate. SEM images of (D) polyXa, (E) polyXa/SWCNT, and (F) polyXa/MWCNT, respectively.

The linear regression equations of peak currents ( $I_{pa}$  &  $I_{pc}$ ) and scan rate ( $\nu$ ) can be expressed as follows:

At polyXa/GCE:

$$I_{pa}(\mu\text{A}) = -0.0152\nu(\text{mV s}^{-1}) - 0.08 \quad (R^2 = 0.9951) \quad (1)$$

$$I_{pc}(\mu\text{A}) = 0.0181\nu(\text{mV s}^{-1}) + 0.10 \quad (R^2 = 0.9952) \quad (2)$$

At polyXa/SWCNT/GCE:

$$I_{pa}(\mu\text{A}) = -0.0952\nu(\text{mV s}^{-1}) - 0.12 \quad (R^2 = 0.9997) \quad (3)$$

$$I_{pc}(\mu\text{A}) = 0.1004\nu(\text{mV s}^{-1}) + 0.12 \quad (R^2 = 0.9998) \quad (4)$$

At polyXa/MWCNT/GCE:

$$I_{pa}(\mu\text{A}) = -0.5988\nu(\text{mV s}^{-1}) - 1.24 \quad (R^2 = 0.9989) \quad (5)$$

$$I_{pc}(\mu\text{A}) = 0.6275\nu(\text{mV s}^{-1}) + 1.27 \quad (R^2 = 0.9989) \quad (6)$$

Moreover, the ratio of oxidation-to-reduction peak currents in each case is nearly unity and formal potentials do not change with increasing scan rate in this pH condition. This result reveals that the electron transfer kinetics is very fast on the electrode modified surface.

We have estimated, the apparent surface coverage ( $\Gamma$ ), by using Eq. (7):

$$I_p = n^2 F^2 \nu A \Gamma / 4RT \quad (7)$$

where,  $I_p$  is the peak current of the polyXa/MWCNT composite electrode;  $n$  is the number of electron transfer;  $F$  is Faraday constant ( $96485 \text{ C mol}^{-1}$ );  $\nu$  is the scan rate ( $\text{mV s}^{-1}$ );  $A$  is the electrode surface area ( $0.07 \text{ cm}^2$ );  $R$  is gas constant ( $8.314 \text{ J mol}^{-1} \text{ K}^{-1}$ ); and  $T$  is the room temperature ( $298.15 \text{ K}$ ). In the present case, the calculated surface coverage ( $\Gamma$ ) was  $6.27 \times 10^{-11} \text{ mol cm}^{-2}$ ,  $3.80 \times 10^{-10} \text{ mol cm}^{-2}$ , and  $2.32 \times 10^{-9} \text{ mol cm}^{-2}$  in a two-electron process for polyXa, polyXa/SWCNT, and polyXa/MWCNT, respectively. One can know that the polyXa/MWCNT shows the higher current response resulted from higher surface coverage. This also indicates that MWCNT provides more active sites for polyXa.

Morphology was studied by scanning electron microscopy (SEM). Fig. 2D–F shows SEM images for polyXa, polyXa/SWCNT, and polyXa/MWCNT, respectively. Fig. 2D displays the polyXa image with fiber-like shape might be due to the formation of polymer chain. Both polyXa/SWCNT (Fig. 2E) and polyXa/MWCNT (Fig. 2F) display globular images might be due to the CNTs aggregation. This result indicates that the composites form their unique structure in the morphology.

### 3.2. Electrocatalytic oxidation of AA, DA, and UA at polyXa-CNTs modified electrodes

Different hybrid films modified electrodes were prepared to study electrocatalytic oxidation of AA, DA, and UA in pH 7 PBS. PolyXa/CNTs show the current response higher than those of CNTs/polyXa hybrid composites. It indicates that polyXa/CNTs are more electroactive than CNTs/polyXa might be due to high compact active species. It may be explained by that the immobilized procedure of first one-dimensional polymer chains and second three-dimensional CNTs might provide the compact and efficient hybrid composites.

### 3.3. Electrocatalytic oxidation of AA, DA, and UA using polyXa-CNTs composites

PolyXa/MWCNT was one of polyXa-CNTs composites used to test single target species (AA, DA, and UA). As shown in Fig. 3A, three well defined oxidation peaks are observed at +0.06 V, +0.28 V, and +0.36 V for AA, DA, and UA, respectively. It proves that polyXa/MWCNT hybrid composite can show specific oxidation peaks for AA, DA, and UA, respectively. Furthermore, the overpotential of AA and UA are similar to the related works [32,33]. It indicates that the hybrid nanocomposite types maintain the electrochemical activities of the electroactive polyXa species.

Different modified electrodes were also examined in the AA, DA, and UA mixing solution, the voltammetric responses were observed to understand their electrocatalytic properties. Fig. 3B shows the cyclic voltammograms of different electrodes in pH 7 PBS containing  $5 \times 10^{-4}$  M AA,  $5 \times 10^{-5}$  M DA, and  $5 \times 10^{-4}$  M UA. Curve (a) shows the voltammogram of bare GCE with only one oxidation peak at about +0.24 V to three target species.

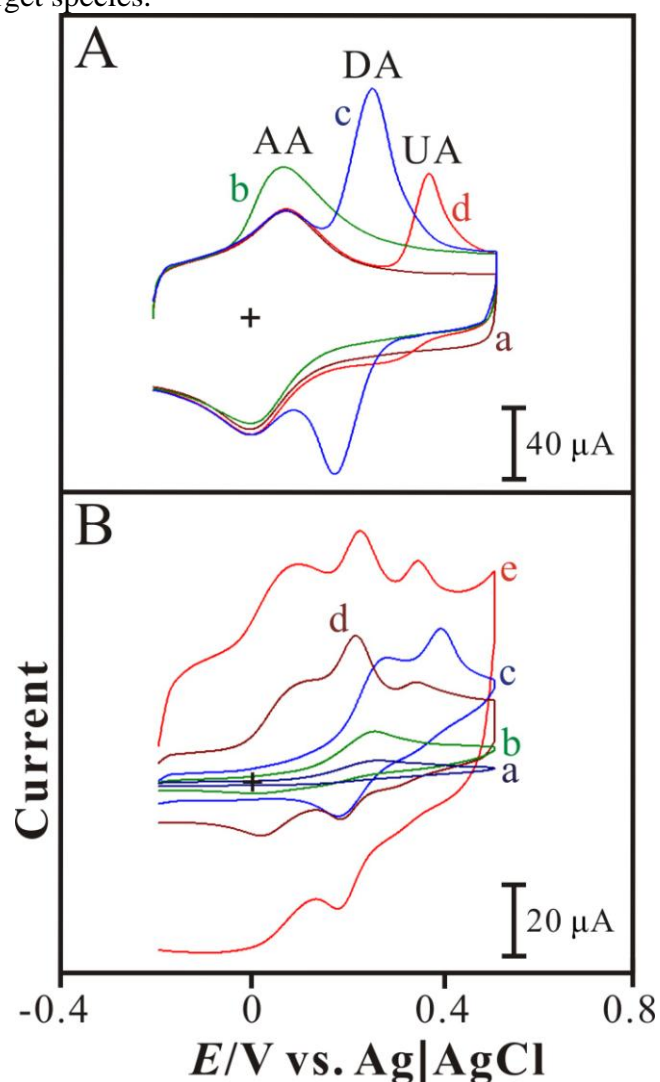


**Figure 3.** (A) CVs of polyXa/MWCNT/GCE examined in 0.1 M PBS (pH 7) containing (a)  $5 \times 10^{-4}$  M AA, (b)  $5 \times 10^{-5}$  M DA, and (c)  $5 \times 10^{-4}$  M UA, respectively. (B) CVs of (a) bare GCE, (b) polyXa/GCE, (c) MWCNT/GCE, (d) polyXa/SWCNT/GCE, and (e) polyXa/MWCNT/GCE examined in 0.1 M PBS (pH 7) containing  $5 \times 10^{-4}$  M AA,  $5 \times 10^{-5}$  M DA, and  $5 \times 10^{-4}$  M UA. Scan rate =  $0.1 \text{ Vs}^{-1}$ .

PolyXa/GCE (curve b) also shows only one oxidation peak similar to that at bare GCE except of higher current. It means that polyXa is active to target species resulted in high current response. However, both bare GCE and polyXa/GCE can't recognize these target species. After the polymer hybridized with CNTs (polyXa/SWCNT or polyXa/MWCNT), it shows significant oxidation peaks (curve d and e). Significant oxidation peaks are observed at  $E_{pa,AA} = +0.08$  V,  $E_{pa,DA} = +0.22$  V, and  $E_{pa,UA} = +0.34$  V. Particularly, curve (e) shows much higher current response indicating that MWCNT-based composite is more active. Considering current response of MWCNT/GCE (Fig. 3B(c)), only two obvious oxidation peaks ( $E_{pa} = +0.270$  V,  $+0.388$  V) are observed for target species. In the contrast, it means that polyXa/CNTs can provide specific electrocatalytic property better than that at MWCNT/GCE or polyXa/GCE. These results also provide the evidence that specific oxidation peaks corresponding to the oxidation of AA, DA, and UA are not only original from MWCNT or polyXa. One can conclude that electrocatalytic oxidation of target species can be improved using the polyXa and CNTs hybrid composites. Particularly, the polyXa/MWCNT hybrid type is more active and can be the candidate to simultaneously determine AA, DA, and UA.

### 3.4. Simultaneous determination of AA, DA, and UA using polyXa/MWCNT

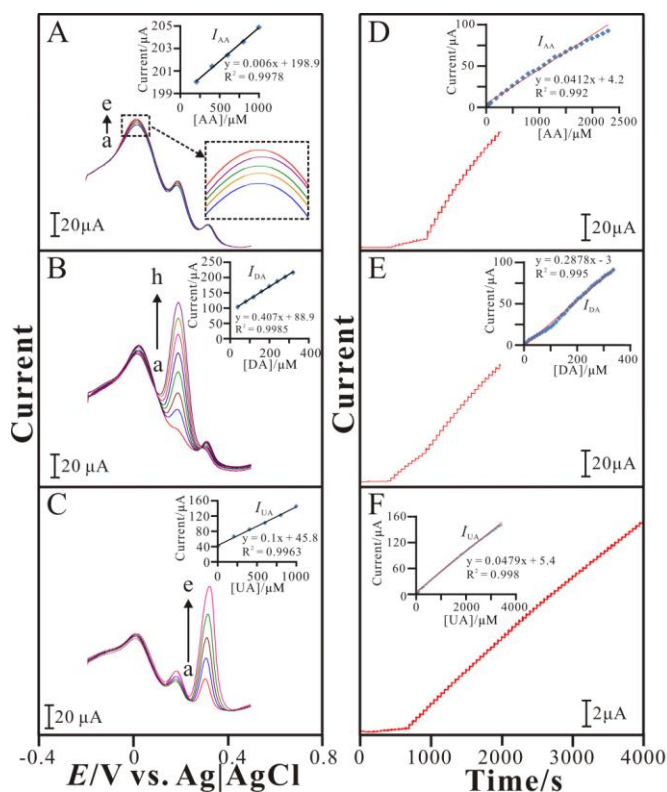


**Figure 4.** DPVs of polyXa/MWCNT/GCE examined for one species determination in pH 7 PBS containing: (A)  $[AA] = (a) 2 \times 10^{-4}$  M – (e)  $1 \times 10^{-3}$  M in the presence of  $8 \times 10^{-5}$  M DA and  $1 \times 10^{-4}$  M UA; and (B)  $[DA] = (a) 4 \times 10^{-5}$  M – (h)  $3.2 \times 10^{-4}$  M in the presence of  $2 \times 10^{-4}$  M AA and  $1 \times 10^{-4}$  M UA; and (C)  $[UA] = (a) 2 \times 10^{-4}$  M – (e)  $1 \times 10^{-3}$  M in the presence of  $1 \times 10^{-4}$  M AA and  $4 \times 10^{-5}$  M DA. Scan rate =  $0.1 \text{ Vs}^{-1}$ . Amperograms of polyXa/MWCNT/GCE applied potential at (D)  $E_{app.} = +0.1$  V, (E)  $E_{app.} = +0.2$  V, and (F)  $E_{app.} = +0.3$  V for AA, DA, and UA, respectively. Electrode rotation speed = 1000 rpm.

Differential pulse voltammetry (DPV) is the electrochemical technique which has much higher current sensitivity and better resolution compared to cyclic voltammetry. Also the contribution of charging current to the background current is negligible in DPV. Therefore, the simultaneous determination of AA, DA and UA at polyXa/MWCNT modified electrode was carried out using DPV technique.

Fig. 4A – C shows the voltammograms of polyXa/MWCNT/GCE used to individually determine AA, DA, and UA in the presence of the other two constant species. Specific oxidation peaks are observed at 11 mV, 181 mV, and 304 mV for AA, DA, and UA, respectively. These oxidation potentials are slightly lower than those in CV results. Peak currents are linearly dependent on concentration, indicating the stable and efficient electrocatalytic activity at the polyXa/MWCNT/GCE by DPV.

Linear regression equation of AA is calibrated as  $I_{AA}(\mu A) = 198.86 + 0.006C_{AA}(\mu M)$  ( $C_{AA}$ : 200–1000  $\mu M$ ) with correlation coefficient of  $R^2 = 0.9978$  ( $n = 5$ ), accompanied with the change of 8.9% and 3.4% for DA and UA. Linear regression equation of DA is calibrated as  $I_{DA}(\mu A) = 88.87 + 0.407C_{DA}(\mu M)$  ( $C_{DA}$ : 40–320  $\mu M$ ) with the correlation coefficient of  $R^2 = 0.9985$  ( $n = 8$ ), accompanied with the change of 11.2% and 5.8% for AA and UA. Linear regression equation of UA is calibrated as  $I_{UA}(\mu A) = 45.76 + 0.1C_{UA}(\mu M)$  ( $C_{UA}$ : 200–1000  $\mu M$ ) with the correlation coefficient of  $R^2 = 0.9963$  ( $n = 5$ ), accompanied with the change of 6.7% and 9.6% for AA and DA. It provides good selectivity and linear concentration range of  $1 \times 10^{-5}$ – $1 \times 10^{-3}$  M,  $1 \times 10^{-5}$ – $3.2 \times 10^{-4}$  M, and  $1 \times 10^{-5}$ – $1 \times 10^{-3}$  M, with detection limit of 10  $\mu M$ , 1  $\mu M$ , and 5  $\mu M$  (S/N= 3). The sensitivity is estimated in 86  $\mu A$  mM  $cm^{-2}$ , 5814  $\mu A$  mM  $cm^{-2}$ , and 1429  $\mu A$  mM  $cm^{-2}$  for AA, DA, and UA, respectively. This result might propose DPV to be the suitable electrochemical technique to determine DA in the presence of AA and UA. The analytical characteristics for the determination of AA, DA, and UA at polyXa/MWCNT/GCE are nearly the same as those obtained in the solution containing only one species, confirming no interference between each other in the measurements.

**Table 1.** Performance of polyXa/MWCNT electrode compared with other modified electrodes for determination of AA, DA, and UA using differential pulse voltammetry (DPV).

Electrode	Linear range ( $\mu M$ )			Detection limit ( $\mu M$ )			Ref.
	AA	DA	UA	AA	DA	UA	
MWCNT/GCE (DPV)	15-800	0.5-100	0.55-90	7.71	0.31	0.42	[13]
PAA-MWCNTs/SPCE (DPV)	100-1000	-	0-30	49.8	-	0.458	[34]
CILE (DPV)	50-7400	2-1500	2-2200	20	1	1	[35]
poly(sulfonazo III)/GCE (DPV)	0.5-1300	0.05-470	0.2-100	0.17	0.03	0.11	[36]
HNCMS/GCE (DPV)	100-1000	3-75	5-30	0.91	0.02	0.04	[37]
PtNPs-MWCNT/GCE (DPV)	24.5-765	0.06-3.02	0.46-50	20	0.05	0.35	[38]
SPGNE (DPV)	4-4500	0.5-2000	0.8-2500	0.95	0.12	0.2	[39]
polyXa/MWCNT/GCE (DPV)	10-1000	10-3200	10-1000	10	1	5	This work
polyXa/MWCNT/GCE (amperometry)	10-2300	5-165	5-1650	10	1	5	This work

Amperometry is one of powerful electrochemical techniques used to determine AA, DA, and UA species. Fig. 4D – F shows the amperometric responses which are evaluated at polyXa/MWCNT/GCE applied potential at +0.1 V, +0.2 V, and +0.3 V for AA, DA, and UA, respectively. Blank signal is obtained in initial 450 seconds. Fig. 4D displays the amperogram with sequential additions of AA ( $10^{-5}$  M per 50 seconds) by micro-syringe. It shows linear concentration range of  $1 \times 10^{-5}$ – $2.3 \times 10^{-3}$  M with sensitivity of  $145.8 \mu\text{A mM}^{-1} \text{cm}^{-2}$  and detection limit of  $10 \mu\text{M}$  ( $S/N = 3$ ). It also provides linear response range of  $5 \times 10^{-6}$ – $1.65 \times 10^{-4}$  M and  $5 \times 10^{-6}$ – $1.65 \times 10^{-3}$  M with sensitivity of  $2036.8 \mu\text{A mM}^{-1} \text{cm}^{-2}$  and  $338.6 \mu\text{A mM}^{-1} \text{cm}^{-2}$  and detection limit of  $1 \mu\text{M}$  and  $5 \mu\text{M}$  ( $S/N = 3$ ) for DA and UA, respectively. Relative standard deviation (RSD) ( $n = 10$ ) is 5.3 %, 3.4 %, and 4.8 % for determining AA, DA, and UA, respectively. It indicates that this sensor has very good reproducibility at pH 7.

Performance is compared with other sensors in the literature (Table 1). It shows wider linear range of AA determination than those of PAA-MWCNTs/SPCE, MWCNT/GCE, HNCMS/GCE, and PtNPs-MWCNT/GCE. Lower detection limit of AA is found better than those of PAA-MWCNTs/SPCE, CILE, and PtNPs-MWCNT/GCE. It also can provide competitive linear range better than that of PAA-MWCNTs/SPCE for UA determination. It can be concluded that polyXa/MWCNT possesses comparable performance for the simultaneous determination of AA, DA, and UA in the literature.

### 3.5. Real sample test

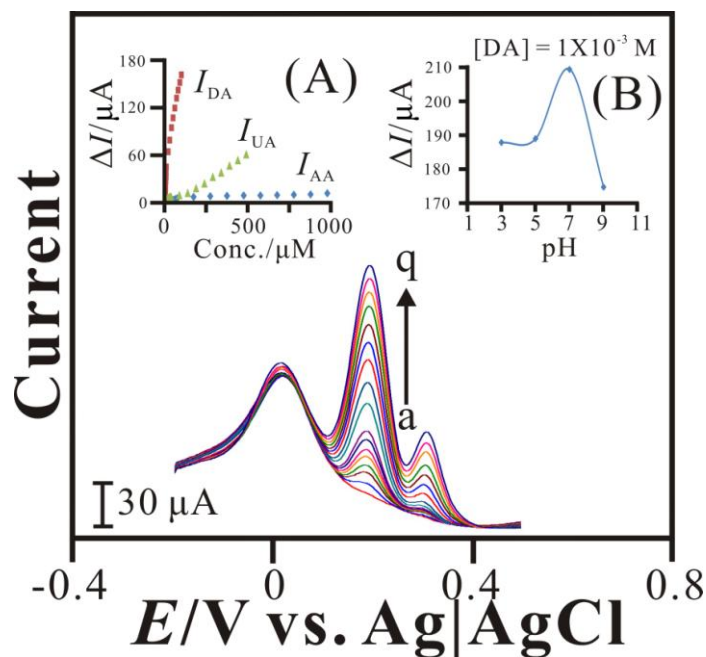


**Figure 5.** Real test in urine sample (pH 7 PBS): DPVs of polyXa/MWCNT/GCE examined with the additional concentration of  $1 \times 10^{-5}$ – $9.7 \times 10^{-4}$  M AA,  $1 \times 10^{-6}$ – $9.7 \times 10^{-5}$  M DA, and  $5 \times 10^{-6}$ – $4.85 \times 10^{-4}$  M UA from case (a) to (q), respectively. Scan rate =  $0.1 \text{ Vs}^{-1}$ . Insets: (A) the plot of peak current change ( $\Delta I$ ) vs. concentration; and (B) the plot of peak current change ( $\Delta I$ ) vs. pH for DA test.

PolyXa/MWCNT modified electrode was further studied for simultaneous determination of AA, DA, and UA in human urine sample by DPV. Prior to the determination, all urine samples were appropriately treated by centrifugation and filtration. Three species were spiked into the electrochemical system with various concentrations. Fig. 5 shows DPV response to AA, DA, and UA with three well-defined oxidation peaks, corresponding to those shown in Fig. 4A–C. Inset A of Fig. 5 depicts the correlation between net current response ( $\Delta I$ ) and species concentration. Linear concentration ranges are estimated in  $1 \times 10^{-5}$ – $9.7 \times 10^{-4}$  M,  $1 \times 10^{-6}$ – $9.7 \times 10^{-5}$  M, and  $5 \times 10^{-6}$ – $4.85 \times 10^{-4}$  M for AA, DA, and UA, respectively. These values are also competitive in the literature as shown in Table 1. Inset B depicts the correlation between net current response ( $\Delta I$ ) and pH condition for DA determination, indicating the optimized condition at pH 7. Real sample analysis provides recovery over than 95% and RSD less than 7% for each case. One can concluded that the sensor shows efficient activity in real sample and can be used for practical examination.

### 3.6. Stability study

Repetitive redox potential cycling experiments were tested to know the extent of stability relevant to polyXa/MWCNT modified electrode in neutral condition. This investigation indicates that after 100 continuous scan cycles with scan rate of  $100 \text{ mV s}^{-1}$ , the peak heights of the cyclic voltammograms decreased less than 5%. A decrease of 8% was observed in current response of the electrode at the end of 10<sup>th</sup> day. One can know that the stability of this electrode which promising it could be used stably for a few days.

## 4. CONCLUSIONS

Here we report a simple method to form a sensor based on polyXa-CNTs hybrid composites. Preparation procedures of these composites are designed and compared for the candidate using for simultaneous determination of AA, DA, and UA. They have good electrocatalytic oxidation for AA, DA, and UA with lower overpotential and higher current response. PolyXa/MWCNT is the composite which shows the better test results when compared with polyXa, polyXa/SWCNT, SWCNT/polyXa, and MWCNT/polyXa. It shows competitive performance for simultaneous determination of AA, DA, and UA in the literature. Particularly, it can also provide good linearity in urine samples. As the results, it is a simple and good strategy due to excellent advantages of fast response, low cost, low overpotential, high current response, high sensitivity, and high selectivity.

### ACKNOWLEDGEMENTS

We acknowledge the Ministry of Science and Technology (Project No. 101-2113-M-027-001-MY3), Taiwan.

### References

1. W. Chen, X. Lin, L. Huang, H. Luo, *Microchim. Acta*, 151 (2005) 101–107.

2. A. Balamurugan, S.M. Chen, *Anal. Chim. Acta*, 596 (2007) 92–98.
3. S. Shahrokhian, H.R. Zare-Mehrjardi, *Sens. Actuators B*, 121 (2007) 530–537.
4. J. Huang, Y. Liu, H. Hou, T. You, *Biosens. Bioelectron.*, 24 (2008) 632–637.
5. P. Shakkthivel, S.M. Chen, *Biosens. Bioelectron.*, 22 (2007) 1680–1687.
6. S. Shahrokhian, M. Ghalkhani, *Electrochim. Acta*, 51 (2006) 2599–2606.
7. M. Noroozifar, M. Khorasani-Motlagh, A. Taheri, *Talanta*, 80 (2010) 1657–1664.
8. Y. Li, X. Lin, *Sens. Actuators B*, 115 (2006) 134–139.
9. A.L. Liu, S.B. Zhang, W. Chen, X.H. Lin, X.H. Xia., *Biosens. Bioelectron.*, 23 (2008) 1488–1495.
10. R.P.D. Silva, A.W.O. Lima, S.H.P. Serrano, *Anal. Chim. Acta*, 612 (2008) 89–98.
11. Y. Liu, J. Huang, H. Hou, T. You, *Electrochem. Commun.*, 10 (2008) 1431–1434.
12. C.L. Sun, H. Lee, J.M. Yang, C.C., Wu *Biosens. Bioelectron.*, 26 (2011) 3450–3455.
13. B. Habibi, M.H. Pournaghi-Azar, *Electrochim. Acta*, 55 (2010) 5492–5498.
14. K.S. Rogers, C. Mohan, *Biochem. Med. Metab. Biol.*, 52 (1994) 10–17.
15. H.Z. Malina, X.D. Martin, *Graefes Arch. Clin. Exp. Ophthalmol.*, 234 (1996) 723–730.
16. G. Thiagarajan, E. Shirao, K. Ando, A. Inoue, D. Balasubramanian, *Photochem. Photobiol.*, 76 (2002) 368–372.
17. K. Murakami, M. Haneda, M. Yoshino, *Biometals*, 19 (2006) 429–435.
18. J. Haccoun, B. Piro, V. Noël, M.C. Pham, *Bioelectrochemistry*, 68 (2006) 218–226.
19. A. Hirano, M. Suzuki, M. Ippommatsu, *J. Electrochem. Soc.*, 139 (1992) 2744–2751.
20. C.E. Banks, R.G. Compton, *Analyst*, 131 (2006) 15–21.
21. C.E. Banks, R.G. Compton, *Analyst*, 130 (2005) 1232–1239.
22. J. Wang, *Electroanalysis*, 17 (2005) 7–14.
23. A.D. Santos, L. Gorton, L.T. Kubota, *Electrochim. Acta*, 47 (2002) 3351–3360.
24. P.R. Lima, W.D.J.R. Santos, A.B. Oliveira, M.O.F. Goulart, L.T. Kubota, *Biosens. Bioelectron.*, 24 (2008) 448–454.
25. M. Santhiago, P.R. Lima, W.D.J.R. Santos, A.B.D. Oliveira, L.T. Kubota, *Electrochim. Acta*, 54 (2009) 6609–6616.
26. G. Milczarek, *Electrochem. Commun.*, 9 (2007) 123–127.
27. F. Pariente, E. Lorenzo, F. Tobalina, H.D. Abruña, *Anal. Chem.*, 67 (1995) 3936–3944.
28. N. Mano, A. Kuhn, *Electrochem. Commun.*, 1 (1999) 497–501.
29. K.C. Lin, T.H. Tsai, S.M. Chen, *Biosens. Bioelectron.*, 26 (2010) 608–614.
30. F.D.A.D.S. Silva, C.B. Lopes, E.D.O. Costa, P.R. Lima, L.T. Kubota, M.O.F. Goulart, *Electrochem. Commun.*, 12 (2010) 450–454.
31. K.C. Lin, Y.S. Li, S.M. Chen, *Sens. Actuators B* 184 (2013) 212–219.
32. F.D.A.D.S. Silva, C.B. Lopes, L.T. Kubota, P.R. Lima, M.O.F. Goulart, *Sens. Actuators B*, 168 (2012) 289–296.
33. K.C. Lin, P.C. Yeh, S.M. Chen, *Int. J. Electrochem. Sci.*, 7 (2012) 12752–12763.
34. S.H. Huang, H.H. Liao, D.H. Chen, *Biosens Bioelectron.*, 25 (2010) 2351–2355.
35. A. Safavi, N. Maleki, O. Moradlou, F. Tajabadi, *Anal. Biochem.*, 359 (2006) 224–229.
36. A.A. Ensafi, M. Taei, T. Khayamian, A. Arabzadeh, *Sens. Actuators B*, 147 (2010) 213–221.
37. C.H. Xiao, X.C. Chu, Y. Yang, X. Li, X.H. Zhang, J.H. Chen, *Biosens. Bioelectron.*, 26 (2011) 2934–2939.
38. Z. Dursun, B. Gelmez, *Electroanalysis*, 22 (2010) 1106–1114.
39. J. Ping, J. Wu, Y. Wang, Y. Ying, *Biosens. Bioelectron.*, 34 (2012) 70–76.